Test Results of the PlessCor APD preamplifier for use in the 50 Mbps Q=4 PPM Receiver

Xiaoli Sun and Frederic M. Davidson

Department of Electrical and Computer Engineering

The Johns Hopkins University

Baltimore, MD 21218

SUMMARY

The APD preamplifier developed by Muoi of PlessCor [1] was fully tested and then incorporated into the 50 Mbps Q=4 PPM receiver reported in [2]. An optical fiber was used to couple the optical signal onto the active surface of the APD, which enabled direct measurement of the optical signal power received by the APD. The 50 Mbps Q=4 PPM receiver with this APD preamplifier achieved a receiver BER of 10^{-6} at a received optical signal power level which corresponded to 36 detected photons per bit, or 0.56nW in average received optical signal power.

April 1991

1. Introduction

Free space optical communication systems require the receiver to be extremely sensitive because of the great distance between satellites. Silicon avalanche photodiodes (APD) can provide the maximum receiver sensitivity because of its internal multication gain. The receiver sensitivity is also limited by the additive thermal noise from the APD preamplifier. This work was to test a custom designed low noise APD preamplifier which had been used in a 325 Mbps NRZ binary OOK optical communication system and had, in 1987, achieved a record receiver sensitivity of 64 detected signal photons per bit under a bit error rate (BER) of 10^{-6} [1][3]. We used this APD preamplifier module in our 50 Mbps Q=4 pulse position modulation (PPM) receiver [2] and the resultant receiver sensitivity increased from 50 detected signal photons per bit [2] to 36 detected signal photons per bit at BER $\leq 10^{-6}$.

A transimpedance amplifier is usually used as the preamplifier with the feedback resistor as the APD load resistor. It can be shown that the spectral density of the current noise which adds to the APD photocurrent is inversely proportional to the feedback resistance. However, the bandwidth of the preamplifier is also approximately equal to reciprocal of the product of the feedback resistance and the shunt capacitance. The major limiting factor to achieve both low noise and wide bandwidth operation is the parasitic shunt capacitance across the feedback resistor which may be reduced by hybrid or integrated circuit technologies.

The APD preamplifier module being tested was made by Dr. Tran Van Muoi of PlessCor Optronics, Inc. It consisted of a low noise APD mounted on a ceramic subcarrier block and a hybrid circuit transimpedance amplifier all in one RF shielded package. The feedback resistance was 5 KΩ and the 3 dB band

width was 220 MHz. The APD ionization coefficient ratio was measured to be k_{eff} =0.008 [1]. This preamplifier was superior to the one we originally used in our 50 Mbps Q=4 PPM receiver which had a feedback resistance of 1.03 KΩ and a 3 dB band width of 440 MHz. The APDs in both module were about the same. Since the 50 Mbps Q=4 PPM receiver required a front end band width of only 200 MHz, the PlessCor APD preamplifier could be substituted and the receiver sensitivity should improve.

Since the APD active surface was about 1 mm back in a small hole on the package, it was difficult to focus the optical signal beam onto the APD active surface and actually measure the total optical power seen by the APD. The method used originally by Muoi was monitoring the APD bias current while lowering the bias voltage to 10 volts [1]. This measurement method might have been inaccurate since it effectively used the APD itself as the optical power meter. An APD at such a low bias voltage was not fully depleted and the quantum efficiency became lower. On the other hand, the APD gain was not necessarily reduce to unity at such a low bias voltage. The measurement result was also affected by the drift of the leakage current of the APD and the biasing circuit. In order to independently and accurately measure the received optical power by the APD, we used a short optical fiber to couple the optical signal to the APD and held the fiber tip as close to the APD active surface as possible. The received optical power could be measured directly by placing the fiber tip in front of an independently calibrated commercial optical power meter.

The details of the measurement of the APD preamplifier parameters is presented in the next section. The measurement results with the 50 Mbps Q=4 PPM receiver is given in Section 3. Section 4 contains some conclusion remarks.

2. Measurement of the APD Preamplifier Parameters

The test setup is shown in Figure 1. The optical fiber used consisted of a two feet plastic optical fiber guide (Fiberguide Industries SFS50/125Y). The diameter of the core was $\phi_{fib}=50\mu m$ and the numerical aperture was NA=0.22±0.02. The diameter of the APD was $\phi_{APD}=500\mu m$. The spot size of the signal beam on the surface the APD can be computed as $\phi_{sig}=2NA\times L+\phi_{fib}$ with L the distance from the fiber tip to the APD surface. Therefore, the APD could capture all the light from the fiber tip as long as $\phi_{sig}<<\phi_{APD}$, or $L<<1mm$. A digital multimeter (DMM) (Fluke 75) and an electrometer (Keithley 617) were used to monitor the APD bias voltage and current. The signal from the preamplifier had to be amplified by another amplifier (MiniCircuit ZFL-1000LN, 0.1-1000MHz, 23.4dB) in order for the PPM receiver to operate properly. Since the output of the preamplifier is inverted, a two way 180° power splitter (MiniCircuit ZFSCJ-2-1) was used to invert the signal again.

Figure 2 is a copy of the schematic circuit diagram of the preamplifier [1]. The front end of the preamplifier consisted of a GaAs MESFET (NE71000). The feedback resistor was $R7=5K\Omega$. The signal was actually AC coupled due to the capacitor, $C3$.

The frequency response of the APD preamplifier module was first measured by biasing the APD close to its break down point and illuminating the APD with CW light (white noise). Figure 3 shows the measured spectral density output from the MiniCircuit amplifier. It shows the preamplifier had a 3 dB band width of about 220 MHz, as reported in [1].

Next, the total dark current (bias current) was measured as a function of the bias voltage under no incident light. The results are plotted in Figure 4. It is noticed that the total measured dark current included both the APD dark

current and the leakage current of the bypass capacitor, $C1$. The leakage current drifted slowly by about 15% as the temperature drifted.

The bias voltage was then fixed at 10 volts and the bias current was measured as a function of the received optical power. The laser transmitter in this measurement was modulated by the 50 Mbps Q=4 PPM encoder. Table 1 lists the measurement results along with the theoretical value (third column) assuming the APD gain equal to unity and the quantum efficiency equal to 80% as Muoi claimed in [1]. The ratio of the measured and the theoretical values are also listed in the fourth column of Table 1. It is seen that the APD biased at 10 volts did not have a unity gain and 80% quantum efficiency as Muoi claimed, at least for 50 Mbps Q=4 PPM signal. If we had measured the received optical power by monitoring the bias current as Muoi did, we would have overestimated the received optical signal power by as much as 80% based on the data shown in Table 1. It might have been possible that the method used by Muoi caused less error for the 325 Mbps NRZ binary OOK signal. The measurement method we used with the optical fiber was much more reliable and accurate than Muoi's method.

The equivalent input noise current spectral density of the preamplifier was determined by measuring the power spectrum of the noise output from the Mini-Circuit amplifier while biasing the APD at 10 volts. The contribution from the APD could be neglected since the APD gain was sufficiently low. The measured average power spectral density was -123 dBm/Hz. The equivalent noise current density can be computed as

$$\frac{d<i_n^2>}{df} = \frac{measured\ power\ density}{amplifier\ gain} \times 50\Omega/(transimpedance\ gain)^2$$

$$= (2.14\ pA/\sqrt{Hz})^2 . \tag{1}$$

The APD bulk leakage current was estimated by increasing the APD gain until the total noise output from the amplifier rose to above the noise floor of the preamplifier itself. The measured power spectral density due to the APD bulk leakage current was about -132 dBm/Hz. The corresponding APD bulk leakage current can be obtained by solving the equation

$$2qFG^2 I_{bulk} \times \frac{R_f^2}{50\Omega} \times amp \ \ gain \ = 132 \ dBm/Hz \qquad (2)$$

where q is the electron charge, G is the average APD gain, F is the APD excess noise factor, I_{bulk} is the APD bulk leakage current, and R_f is the feedback resistance of the transimpedance preamplifier. The APD gain was obtained by measuring the pulse amplitude output from the preamplifier in response to a pulsed incident optical signal. The value of the APD gain can be determined by solving the equation

$$V_{pk} = G \frac{\eta P_{spk}}{hf} qR_f \qquad (3)$$

where V_{kp} is the measured pulse amplitude output from the preamplifier, η is the APD quantum efficiency, P_{spk} is the received peak optical power, and hf is the photon energy. The APD gain was found to be G=540 and the APD excess noise factor was $F = GK_{eff} + (2-1/G)(1-k_{eff}) = 6.32$. The APD bulk leakage current was then $I_{bulk} = 0.98 \ pA$ according to (2). Although the APD surface leakage current could not be measured, its contribution to the total noise could be neglected.

It is noticed that the measurement results reported in this section were only rough estimates. We assumed the noise spectral density was constant and used a RF spectrum analyzer to measure the average noise density. In practice, the noise spectrum was not constant and fluctuated over the frequency range.

Furthermore, the measured noise spectral noise densities were close to the noise floor of the spectrum analyzer.

3. Use of the APD Preamplifier in the 50 Mbps Q=4 PPM Receiver

The receiver BER of the 50 Mbps Q=4 PPM receiver was measured as a function of the received optical signal level in terms of number of detected signal photons per information bit defined as

$$Photons/bit = \frac{\eta P_{av} T_w}{hf} \tag{4}$$

with P_{av} the measured average optical power and T_w=40ns the PPM word interval. Figure 5 shows the measurement results. The APD gain was optimized near $BER \approx 10^{-6}$, by adjusting the APD bias voltage until the receiver BER was minimized for a fixed received optical signal level. The value of the optimal APD gain was measured to be G=310 using the method described in the previous section. Figure 5 shows that the receiver with this APD preamplifier achieved a receiver BER of 10^{-6} at 36 detected signal photons per bit (0.56nW or -62.5dBm). The theoretically predicted value of the optimal APD gain was G=250 based on the APD and preamplifier parameters extracted in the previous section. Figure 5 also shows the the theoretically predicted receiver BER vs. photons per bit which was computed using the algorithm described in [4]. The measured data was close to that predicted by the theory. Unfortunately, the APD active surface was damaged after this set of measurement due to the occasional contact by the optical fiber tip. There was no protective glass window in front of the APD active surface.

4. Discussions

The custom designed APD preamplifier was shown to have an equivalent input noise current density of 2.14 pA/$\sqrt{\text{Hz}}$ as compared to 7.7pA/$\sqrt{\text{Hz}}$ for the preamplifier we originally used in our 50 Mbps Q=4 PPM receiver. The bandwidth of the preamplifier was found to be 220 MHz which was just sufficient for the 50 Mbps Q=4 PPM signal. The APD contained in the APD preamplifier module was similar to the one we originally used except for a larger bulk leakage current, 0.98 pA as compared to 0.10 pA. The overall receiver sensitivity when using the custom designed APD preamplifier module was improved by about 1.4 dB, to 36 detected signal photons per bit at $BER \leq 10^{-6}$. The best receiver performance reported so far for similar systems was 39 photons per bit which was achieved by using a state-of-the-art APD ($Slik$ APD, k_{eff} =0.005 [5]). Our receiver sensitivity is expected to further improve if we use a $Slik$ APD with the custom designed preamplifier.

We have used an optical fiber to couple the optical signal to the APD, which provided a direct and reliable way to measure the received optical signal power. The method used by Muoi in which the APD itself was used as an optical power meter was shown to be very unreliable.

The electrical bandwidth of this APD preamplifier is not sufficient for higher data rate Q=4 PPM receivers, for example, 220 Mbps or 325 Mbps. However, GaAs transimpedance amplifiers commercially available today can have similar spectral noise current density but a much wide bandwidth (e.g. GigaBit Logic 16G071-30L1, 700 MHz, 3.0pA/$\sqrt{\text{Hz}}$ [6]). A $Slik$ APD and an integrated circuit GaAs transimpedance amplifier, such as GigaBit Logic 16G071 or 16G072, should be used in a high data rate Q=4 PPM receiver (e.g. 220 Mbps) in order to achieve the highest receiver sensitivity.

References

[1] T. V. Muoi, 'Extremely sensitive receiver for laser communications,' final report prepared for NASA Goddard Flight Center, Greenbelt MD 20771, under contract No. NAS5-29283, PlessCor Optronics, Inc. 20200 Sunburst St., Chatsworth, CA 91311-6289.

[2] X. Sun, F. Davidson, and C. Field, '50 Mbps free space direct detection laser diode optical communication system with Q=4 PPM signaling,' in *Free-Space Laser Communication Technologies II*, D. Begley and B. Seery editors, SPIE proceedings, Vol. 1218, pp. 385-395, January 1990.

[3] T. V. Muoi, 'Extremely sensitive direct detection receiver for laser communications,' *Conference on Lasers and Electro-Optics (CLEO'87)*, Technical Digest Series, Vol. 9, pp. 302-304, Paper THS4.

[4] F. M. Davidson and X. Sun, 'Gaussian approximation versus nearly exact performance analysis of optical communication systems with PPM signaling and APD receivers,' *IEEE Trans. Commun.*, Vol. COM-36, No. 11, pp. 1185-1192, Nov. 1988.

[5] A. D. MacGregor, B. Dion, C. Noldeke, and O. Duchmann, '39 photons/bit direct detection receiver at 810 nm, BER= 1×10^{-6}, 60 Mb/s QPPM,' in *Free-Space Laser Communication Technology III*, David L. Begley and Bernard D. Serry, editors, proc. SPIE 1417-52, 1991.

[6] *GigaBit Logic 1991 GaAs IC Data Book & Designer's Guide*, GigaBit Logic Inc., Newbury Park, CA, August 1990.

P_{in}	$I_{measure}$	I_{theory}	$I_{measure}/I_{theory}$
5.0nW	5nA	2.65nA	1.89
6.0nW	5nA	3.18nA	1.57
52.6nW	48nA	27.9nA	1.72
53.6nW	37.3nA	28.4nA	1.31
429nW	352nA	227nA	1.55
434nW	315nA	230nA	1.47
450nW	400nA	238nA	1.68
3.9μW	3.5μA	2.07μA	1.69
30μW	28.6μA	15.9μA	1.80

Table 1. Measured APD photocurrent, $I_{measured}$, as a function of the average received power, P_{in}, of the 50 Mbps Q=4 PPM optical signal.
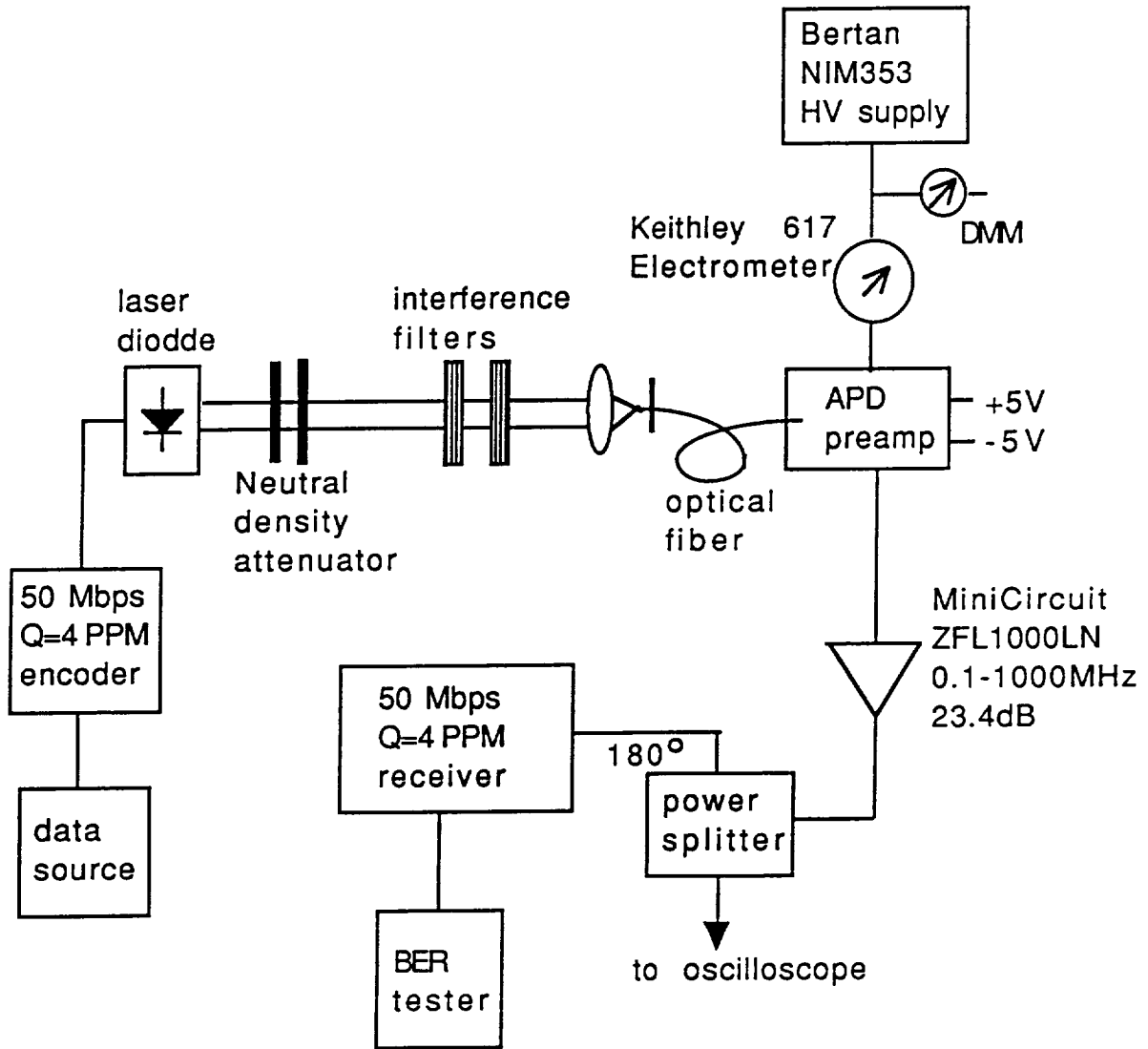
Figure 1. Test setup.
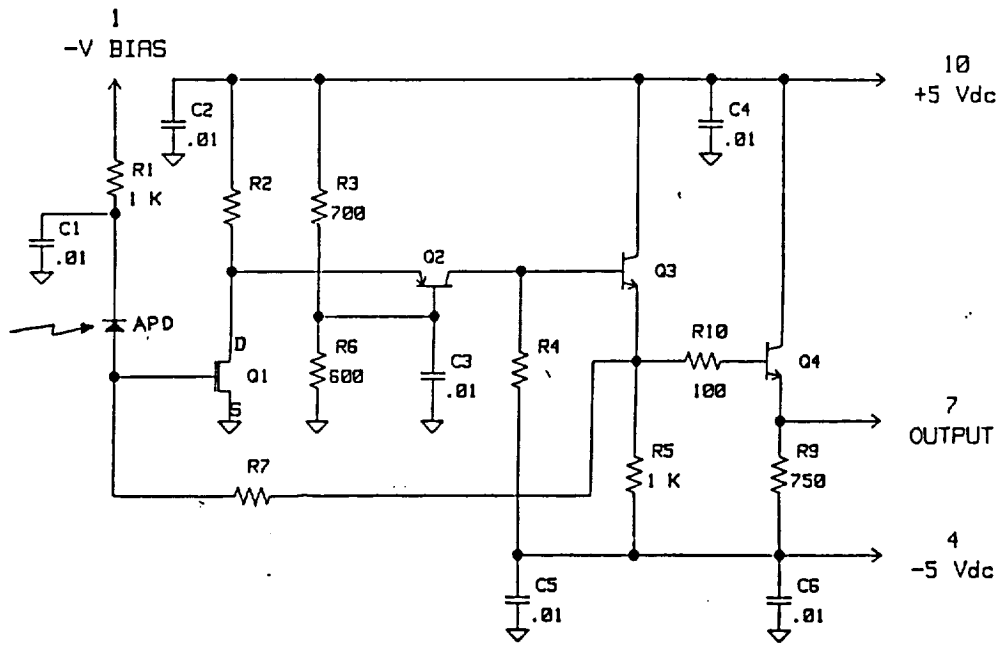
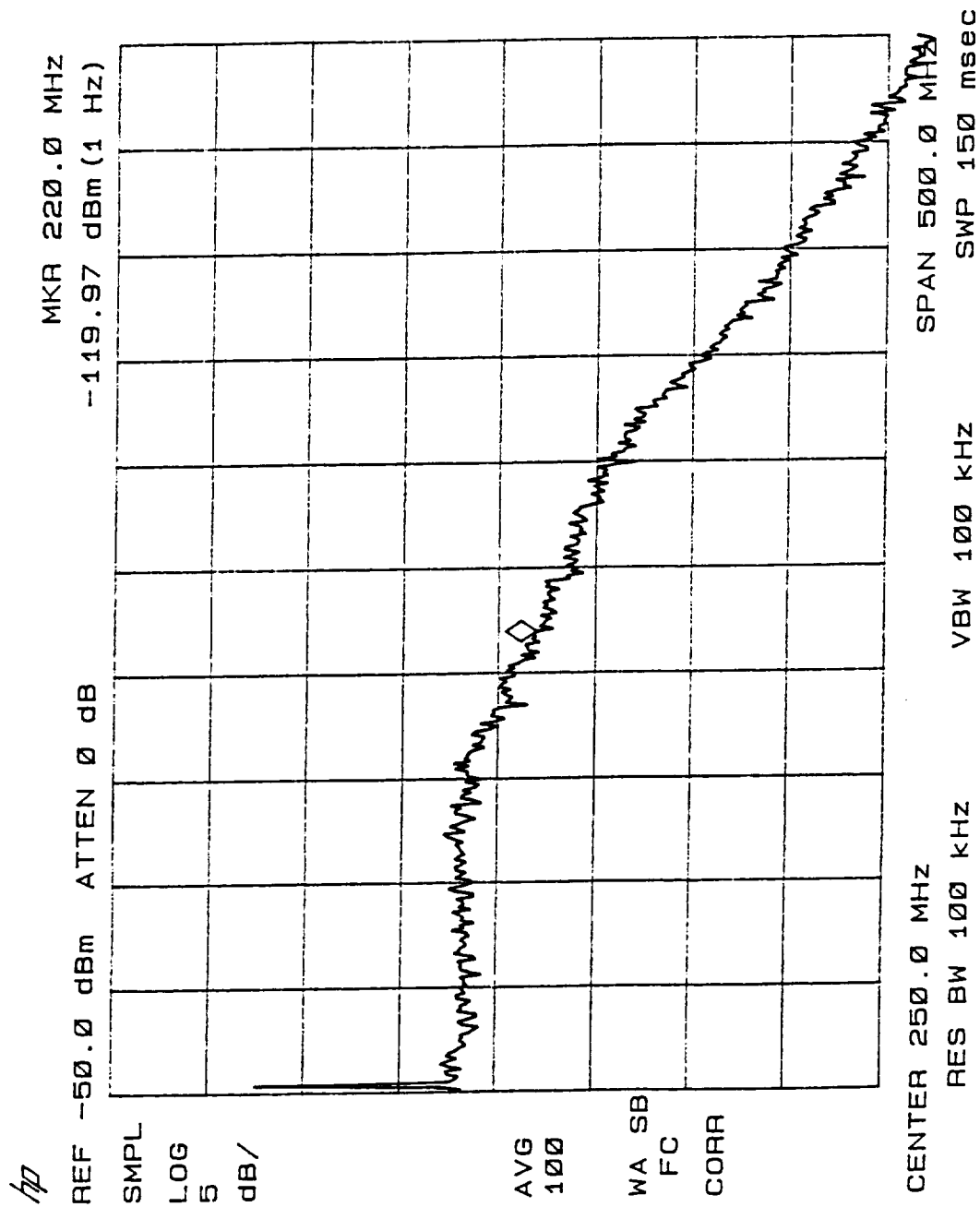Figure 2. Circuit diagram of the PlessCor APD preamplifier.

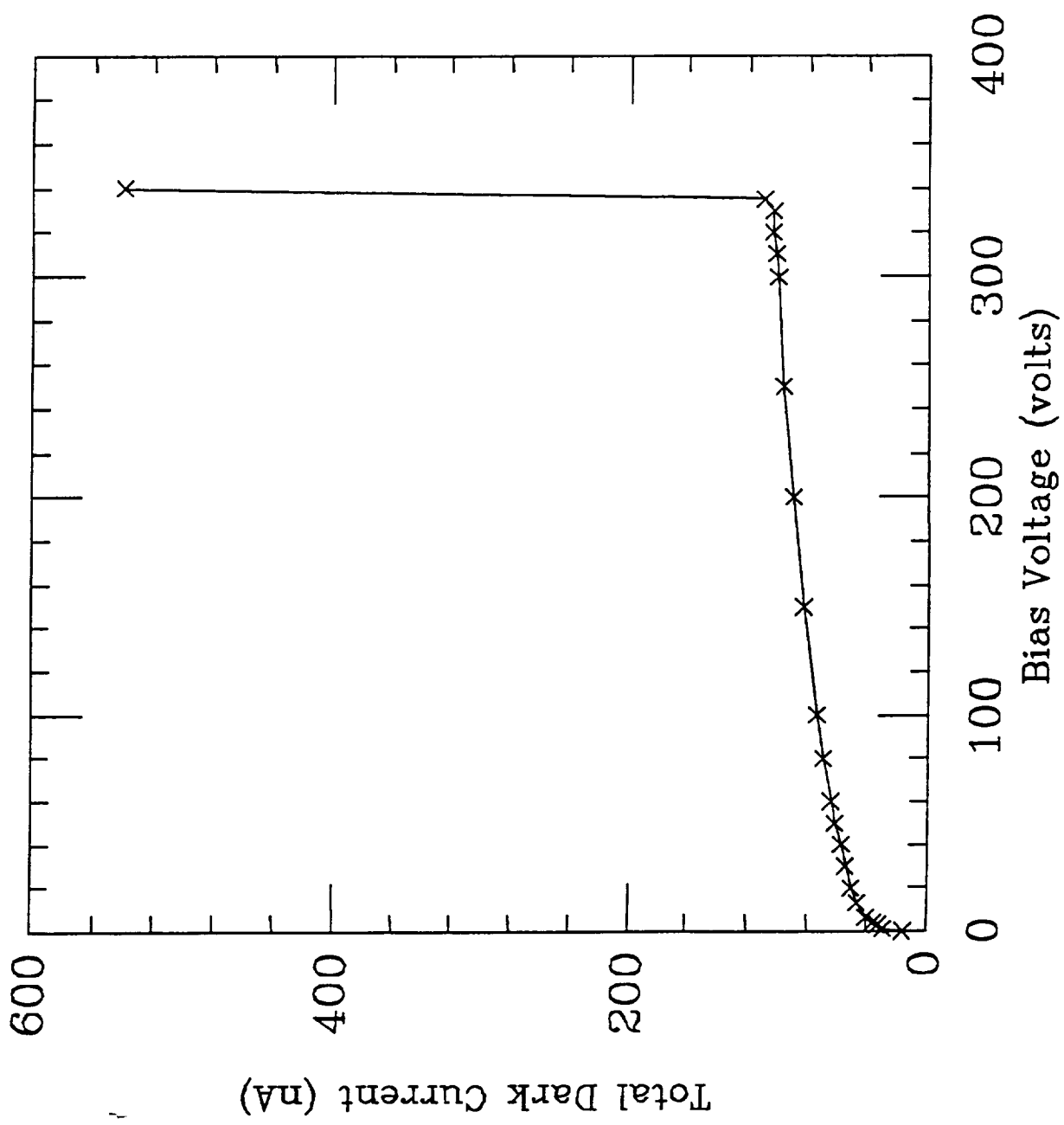Figure 3. Frequency response of the preamplifier.

Figure 4. Measured total dark current (bias current) as a function of the bias voltage applied across the APD.
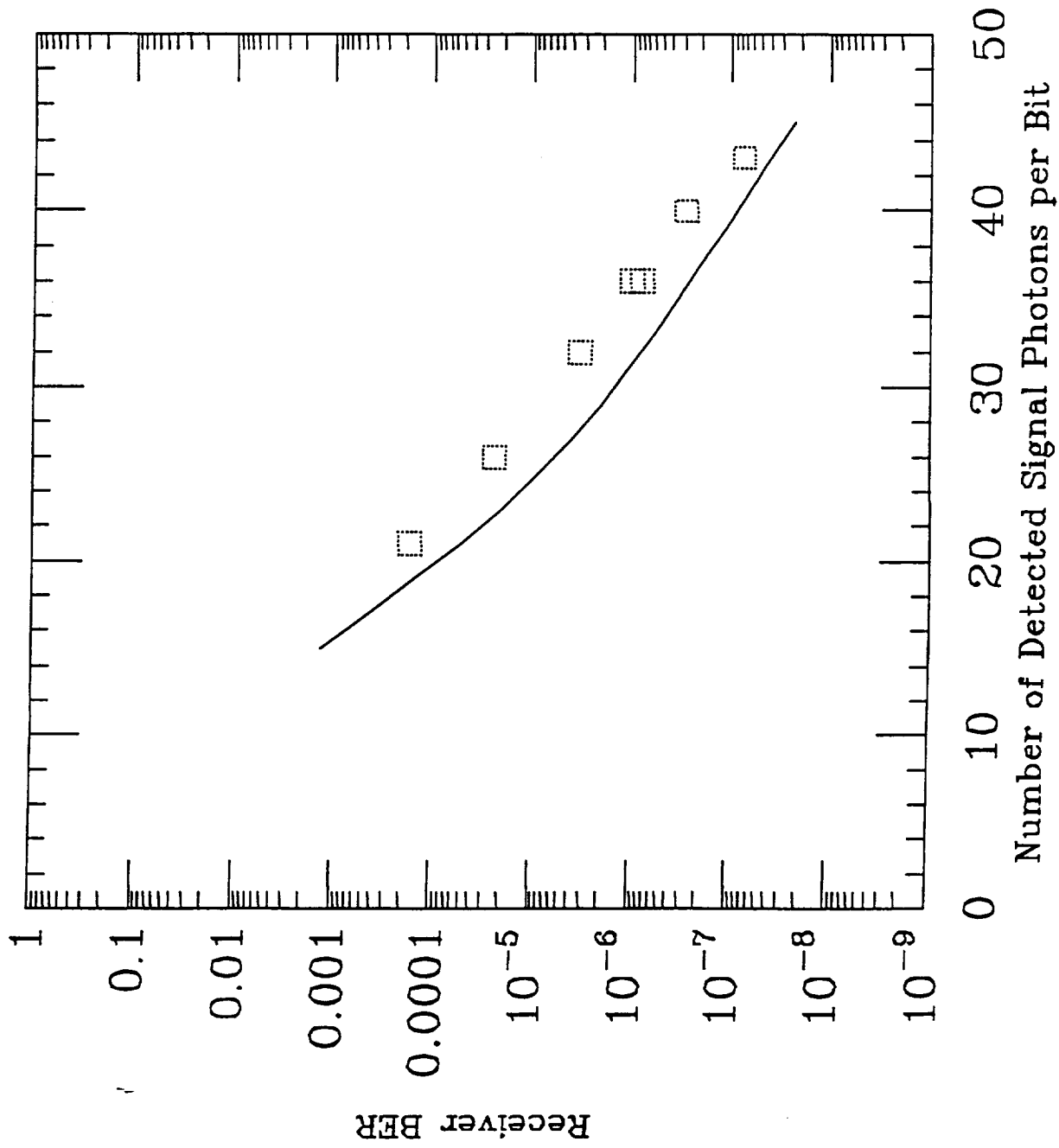
Figure 5. Receiver BER vs. the average received optical power in terms of average number of detected signal photons per information bit.

Q= 4 PPM Signaling

MBPS	NBG	EXTR	KEFF	IS	IB	RLOAD	NTEMP
50.	0.000	0.100E+07	0.008	0.15E-07	0.98E-12	5000.	415.

APDgain	Photons/bit	Pav(nW)	BER
300.	15	0.227	0.1325E-02
300.	17	0.257	0.4424E-03
300.	19	0.287	0.1494E-03
300.	21	0.318	0.5267E-04
300.	23	0.348	0.2008E-04
300.	25	0.378	0.8488E-05
300.	27	0.408	0.3979E-05
300.	29	0.439	0.2025E-05
300.	31	0.469	0.1090E-05
300.	33	0.499	0.6065E-06
300.	35	0.529	0.3443E-06
300.	37	0.560	0.1978E-06
300.	39	0.590	0.1147E-06
300.	41	0.620	0.6677E-07
300.	43	0.650	0.3912E-07
300.	45	0.681	0.2291E-07
300.	47	0.711	0.1353E-07
300.	49	0.741	0.8011E-08
300.	51	0.772	0.4683E-08
300.	53	0.802	0.2790E-08
300.	55	0.832	0.1666E-08
300.	57	0.862	0.9364E-09
300.	59	0.893	0.5620E-09
300.	61	0.923	0.3379E-09
300.	63	0.953	0.2035E-09
300.	65	0.983	0.9725E-10

Memorandum

From: Xiaoli Sun, Department of ECE, Johns Hopkins University

to: James M. Budinger and Jama Mohammed
        NASA/Lewis Research Center, Code MS 54-8

Date: June 13, 1991

Performance of Q-ary PPM receiver
under Additive White Gaussian Noise

1. Introduction

One way to test the circuit of a Q-ary PPM receiver in an optical intersatellite link is to measure the receiver performance under a known injected additive white Gaussian noise (AWGN). It is only an indirect test since the shot noise generated by a photodetector is not additive but multiplicative. The receiver performance will be different under different type of noises. Nevertheless, we can still test if the circuit behaves as expected in the case of AWGN injection.

If we assume the receiver to be tested does not include the photodetector and the preamplifier, the input signal level is normally relatively high and the thermal noise of the circuit itself should be negligible. However, there may be some other noise sources, such as timing misalignment or jitter, which may affect the receiver performance. The effect of these noise source can be determined by comparing the measured receiver performance to the theoretically predicted performance of an ideal receiver under the same amount of injected AWGN. The degradation of the receiver performance due to noises other than the injected can then be assessed. The receiver circuit may cause about the same amount of degradation when it is used with a photodetector.

The rest of this memo gives a theoretical performance analysis of an ideal receiver under AWGN injection.

2. BER vs. SNR when using ML detection

ML detection is to compare the receiver output at the end of each slot within a PPM word to find the largest. The receiver BER is related to PPM word error rate (WER) by [1]

$$BER = \frac{Q}{2(Q-1)} \times WER \qquad (1)$$

The signal output from a matched filter is a Gaussian r.v. and the mean and variance are given by [2]

$$\mu = \begin{cases} E, & \text{pulse present} \\ 0, & \text{pulse absent} \end{cases} \qquad (2)$$

$$\sigma^2 = \sqrt{N_0 E / 2} \qquad (3)$$

where $E =$ pulse energy, and $N_0 =$ one sided noise spectral density. It can be shown that [2]

$$WER_{ML} = 1 - \int_{-\infty}^{\infty} \frac{1}{\sqrt{2\pi}} e^{-z^2/2} \left[\int_{-\infty}^{z+(2E/N_o)^{1/2}} \frac{1}{\sqrt{2\pi}} e^{-u^2/2} du \right]^{Q-1} dz \quad . \qquad (4)$$

The relative accuracy required for the integral in (4) is impractical since we are only interested in small value of WER_{ML} and the integral in (4) is very close to unity. We may rewrite (4), to a good approximation, as

$$WER_{ML} \approx (Q-1) \int_{-\infty}^{\infty} \frac{1}{\sqrt{2\pi}} e^{-z^2/2} \left[\int_{z+(2E/N_o)^{1/2}}^{\infty} \frac{1}{\sqrt{2\pi}} e^{-u^2/2} du \right] dz$$

$$= \frac{Q-1}{2} \frac{1}{\sqrt{\pi}} \int_{-\infty}^{\infty} e^{-u^2} erfc(u + \sqrt{E/N_o}) du \qquad (5)$$

where $erfc(v) = (2/\sqrt{\pi}) \int_{0}^{v} e^{-v^2} dv$ is the complimentary error function.

3. BER vs. E/N sub o when using threshold crossing detection

Threshold crossing detection is to compare the signal output from the matched filter against a threshold at the end of each PPM slot.

$$WER_{th} = 1 - (1 - P_{fa})^{Q-1}(1 - P_{ms}) \approx P_{ms} + (Q-1)P_{fa}$$

$$= \int_{-\infty}^{th} p_1(x)dx + (Q-1)\int_{th}^{\infty} p_0(x)dx \tag{6}$$

Optimal threshold is the solution to:

$$\frac{dWER_{th}}{dth} = 0 \quad \rightarrow \quad p_1(th_{opt}) = (Q-1)p_0(th_{opt})$$

It can be shown that

$$th_{opt} = \frac{E}{2} + \frac{N_0}{4}\ln(Q-1) = \frac{E}{2}[1 + \frac{1}{2E/N_o}ln(Q-1)] \tag{7}$$

and

$$WER_{th} = \frac{1}{2}erfc\{\frac{1}{2}\sqrt{E/N_o}\ [1 - \frac{1}{2E/N_o}ln(Q-1)]\ \}$$

$$+ \frac{(Q-1)}{2}erfc\{\frac{1}{2}\sqrt{E/N_o}\ [1 + \frac{1}{2E/N_o}ln(Q-1)]\ \} . \tag{8}$$

If we fix the threshold to $th = E/2$, then $P_{ms} = P_{fa}$ and

$$WER_{th}' = QP_{ms} = Q\int_{-\infty}^{-\sqrt{E/2N_o}} \frac{1}{\sqrt{2\pi}}e^{-z^2/2}dz = \frac{Q}{2}erfc(\frac{1}{2}\sqrt{E/N_o}) . \tag{9}$$

4. Numerical results

A computer program was written to evaluate (5), (8), and (9) assuming $Q = 4$ PPM signal format. The results and the computer program used are given as the attached.

References

[1] A. J. Viterbi, *Principles of Coherent Communication*, New York: McGraw-Hill, 1966, ch. 8, p. 226.

[2] A. D. Whalen, *Detection of Signals in Noise*, New York: Academic Press, 1971, ch. 6, p. 182.
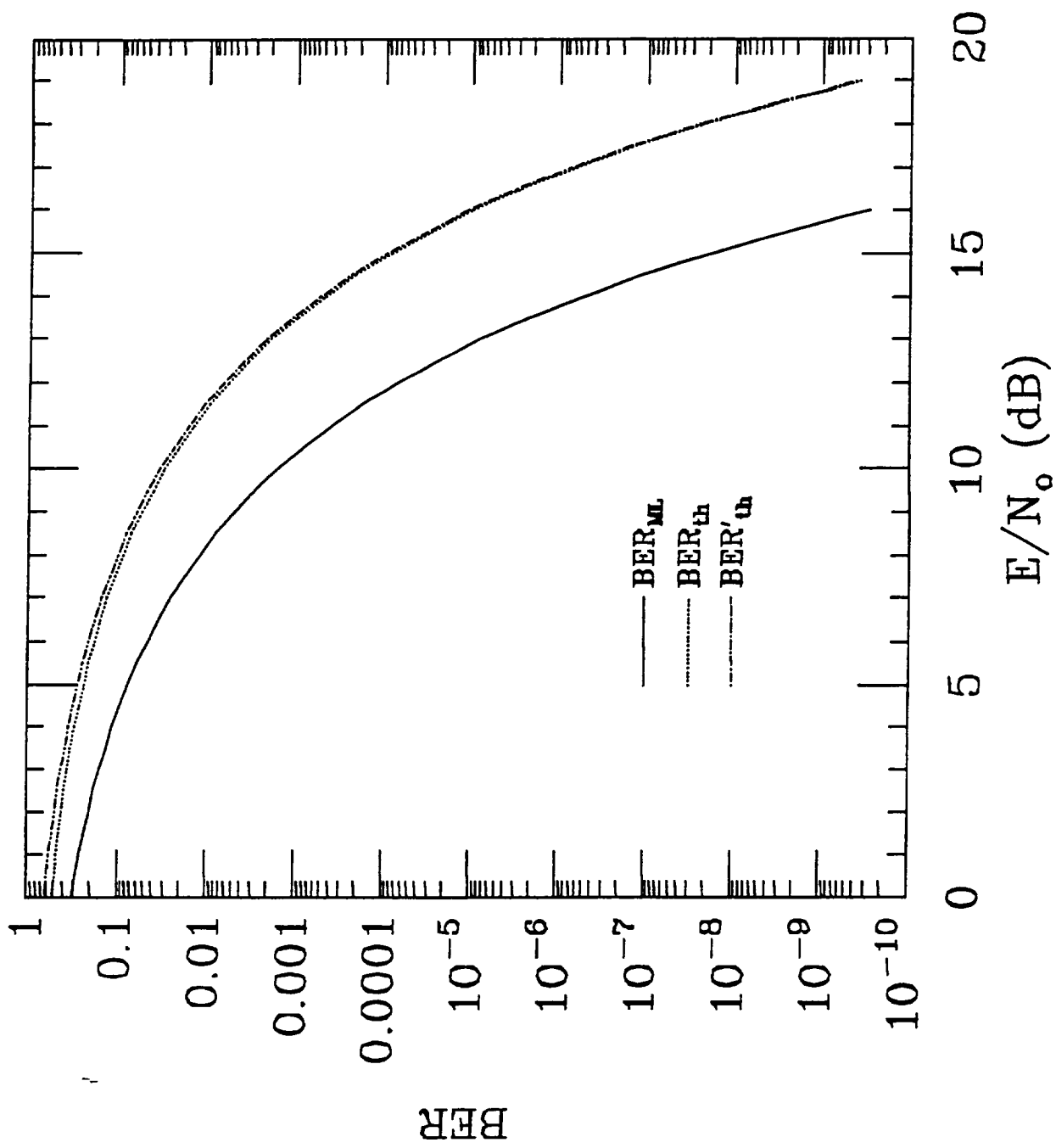
SNR(dB)	SNR(real)	BERms	BERthopt	BERthl/2
0.00	1.0000	3.173e-01	5.233e-01	6.393e-01
0.50	1.1220	2.895e-01	4.986e-01	6.051e-01
1.00	1.2589	2.619e-01	4.727e-01	5.701e-01
1.50	1.4125	2.346e-01	4.456e-01	5.342e-01
2.00	1.5849	2.081e-01	4.176e-01	4.978e-01
2.50	1.7783	1.824e-01	3.887e-01	4.609e-01
3.00	1.9953	1.578e-01	3.591e-01	4.238e-01
3.50	2.2387	1.346e-01	3.292e-01	3.867e-01
4.00	2.5119	1.130e-01	2.991e-01	3.499e-01
4.50	2.8184	9.319e-02	2.691e-01	3.136e-01
5.00	3.1623	7.536e-02	2.396e-01	2.781e-01
5.50	3.5481	5.961e-02	2.108e-01	2.438e-01
6.00	3.9811	4.601e-02	1.830e-01	2.110e-01
6.50	4.4668	3.456e-02	1.566e-01	1.801e-01
7.00	5.0119	2.517e-02	1.319e-01	1.512e-01
7.50	5.6234	1.772e-02	1.091e-01	1.248e-01
8.00	6.3096	1.201e-02	8.847e-02	1.009e-01
8.50	7.0795	7.797e-03	7.018e-02	7.989e-02
9.00	7.9433	4.827e-03	5.431e-02	6.170e-02
9.50	8.9125	2.832e-03	4.089e-02	4.636e-02
10.00	10.0000	1.565e-03	2.986e-02	3.380e-02
10.50	11.2202	8.091e-04	2.107e-02	2.381e-02
11.00	12.5893	3.880e-04	1.431e-02	1.615e-02
11.50	14.1254	1.710e-04	9.311e-03	1.049e-02
12.00	15.8489	6.861e-05	5.777e-03	6.503e-03
12.50	17.7828	2.476e-05	3.398e-03	3.820e-03
13.00	19.9526	7.938e-06	1.882e-03	2.114e-03
13.50	22.3872	2.229e-06	9.752e-04	1.094e-03
14.00	25.1189	5.390e-07	4.688e-04	5.256e-04
14.50	28.1838	1.103e-07	2.072e-04	2.321e-04
15.00	31.6228	1.872e-08	8.334e-05	9.331e-05
15.50	35.4813	2.575e-09	3.017e-05	3.375e-05
16.00	39.8107	2.798e-10	9.703e-06	1.085e-05
16.50	44.6684	2.334e-11	2.733e-06	3.055e-06
17.00	50.1187	1.447e-12	6.635e-07	7.412e-07
17.50	56.2341	6.433e-14	1.364e-07	1.523e-07
18.00	63.0957	1.969e-15	2.324e-08	2.594e-08
18.50	70.7946	3.964e-17	3.213e-09	3.585e-09
19.00	79.4328	4.989e-19	3.510e-10	3.915e-10
19.50	89.1251	3.706e-21	2.946e-11	3.285e-11
20.00	100.0000	1.524e-23	1.839e-12	2.050e-12

```c
#include <stdio.h>
#include <math.h>

#define Q 4

float qtrap(), trapzd(), pr() ;
static double rtsnr;

main()
{
int i;
double snr0, snr1, dsnr, snr, rsnr ;
float BERml, WERml, BERth, WERth, BERoth, WERoth ;

printf("SNR from ? to ? (dB)\n");
scanf("%lf", &snr0 );
scanf("%lf", &snr1 );
dsnr = (snr1-snr0)/40.0;

for( i=0; i<=40; ++i )
   {
      snr = snr0 + i*dsnr ;
      rsnr = exp( snr/10.0 * log(10.0) );
      rtsnr= sqrt(rsnr);

      WERml= 1/sqrt(M_PI) * (Q-1)/2.0 * qtrap( pr, -10.0, 10.0);
      BERml=Q/2.0/(Q-1)*WERml;

      WERoth= 0.5 * erfc( 0.5*rtsnr*(1.0-log(3.0)/2.0/rsnr) )
                  + (Q-1) * 0.5 * erfc( 0.5*rtsnr*(1.0+log(3.0)/2.0/rsnr) );
      BERoth=Q/2.0/(Q-1)*WERoth;

      WERth = Q * 0.5 * erfc( 0.5*rtsnr );
      BERth=Q/2.0/(Q-1)*WERth;

      printf("%8.2f %10.4f %15.3e %15.3e %15.3e \n",
                              snr, rsnr, BERml, BERoth, BERth );

   }
}

/* The integrand */

float pr(u)
double u ;
{
return exp( -u*u ) * erfc( u + rtsnr ) ;
}
```

```c
#include <math.h>
#include <stdio.h>

#define EPS 1.0e-3
#define JMAX 20

float qtrap(func,a,b)
float a,b;
float (*func)();
{
        int j;
        float s,olds,trapzd();
        void nrerror();

        olds = -1.0e30;
        for (j=1;j<=JMAX;j++) {
                s=trapzd(func,a,b,j);
                if (fabs(s-olds) < EPS*fabs(olds)) return s;
                olds=s;
        }
        nrerror("Too many steps in routine QTRAP");
}

#undef EPS
#undef JMAX

void nrerror(error_text)
char error_text[];
{
        void exit();

        fprintf(stderr,"Numerical Recipes run-time error...\n");
        fprintf(stderr,"%s\n",error_text);
        fprintf(stderr,"...now exiting to system...\n");
        exit(1);
}
```

```c
#define FUNC(x) ((*func)(x))

float trapzd(func,a,b,n)
float a,b;
float (*func)();              /* ANSI: float (*func)(float); */
int n;
{
        float x,tnm,sum,del;
        static float s;
        static int it;
        int j;

        if (n == 1) {
                it=1;
                return (s=0.5*(b-a)*(FUNC(a)+FUNC(b)));
        } else {
                tnm=it;
                del=(b-a)/tnm;
                x=a+0.5*del;
                for (sum=0.0,j=1;j<=it;j++,x+=del) sum += FUNC(x);
                it *= 2;
                s=0.5*(s+(b-a)*sum/tnm);
                return s;
        }
}
```

Use of a Bessel Lowpass Filter
as an Approximate Raised Cosine Filter.

Xiaoli Sun

Department of Electrical and Computer Engineering
The Johns Hopkins University
Baltimore, Maryland, 21218

Direct detection free space optical communication systems are now being developed as the first generation optical intersatellite links. Quarternary pulse position modulation (QPPM) format is preferred because of the relatively simple maximum likelihood detection circuit, higher receiver sensitivity, and constant laser duty cycle. A maximum likelihood QPPM receiver contains a filter which integrates received signal over each QPPM time slot. The receiver frontend electrical bandwidth has to be at least four times the source binary data rate in order to give a satisfactory receiver performance. It has been shown that a raised cosine filter may be substituted for the integrator to reduce the receiver frontend bandwidth to no more than two times the source binary data rate. The penalty in receiver sensitivity when using a raised cosine filter is only about 0.5 dB in terms of the input optical signal power required to achieve a bit error rate (BER) of 10^{-6}. A complete theoretical analysis of the receiver performance when using a raised cosine filter can be found in [1].

A raised cosine filter with trapezoidal input pulses is in fact a type of lowpass filter which has a linear phase response. The frequency response of a raised filter with $\beta=1$ is especially close to that of an ordinary lowpass filter [1]. One can circumvent the difficulties in the analytical derivation of the exact raised cosine filter by using a lowpass filter with similar frequency response. A Bessel lowpass filter can be used as an approximate raised cosine filter since Bessel filters give maximum flat phase delay [2]. Other type of well known lowpass filters such as Butterworth and Chebychev filters are not considered here since they tend to have very nonlinear phase responses near the cutoff frequency. A Bessel lowpass filter

can be implemented as a ladder network of capacitors and inductors [2]. The number of capacitors and inductors required and their values can be determined via table look-up once the order and the 3 dB cutoff frequency of the filter are known.

A computer program was written to find the optimal values of the order and the 3 dB cutoff frequency of the Bessel lowpass filter. The program was written in LabView by National Instrument, Austin, Texas, and the computer used was a McIntosh IIci. The LabView software contains a library of filter subroutines including Bessel lowpass filters. The program can simulate the filter output for any given input pulse shape through digital signal processing. The optimal values of the order and 3 dB cutoff frequency of the Bessel lowpass filter are such that the simulated output is the closest to the exact raised cosine pulse shape. The input to the Bessel lowpass filter being designed consists of either computer generated rectangular pulses or actual pulses output from the photodetector preamplifier acquired via an IEEE-488 bus.

A detailed block diagram of the program is shown in Figure 1. The actual pulses is first displayed on a digitizing oscilloscope (Tektronic 11402) which is used as a waveform digitizer. The displayed waveform is then sent to the computer via an IEEE-488 interfacing bus. This part of the program has been successfully tested but not yet integrated into the main program at this time. The results described in this report were obtained using the computer generated rectangular pulse shapes. The computer generated rectangular waveform is first passed through a RC lowpass filter which simulates the preamplifier and then a RC highpass filter which simulates the AC coupling between the amplifiers at the front end of the receiver.

The program used the normalized time scale, i.e., assuming the input pulsewidth is one second. The results could be scaled down to the actual time scale. The number of samples per pulsewidth was set to 200. The rise and fall times of the_ rectangular pulses were 20% of the pulsewidth. The preamplifier 3 dB bandwidth was equal to the reciprocal of the pulsewidth. A printout of the program is shown in Figure 2.

In general, the higher the order of the Bessel lowpass filter, the more symmetric the output pulse shape. The higher the 3 dB cutoff frequency, the narrower the output pulse shape. However, the order and the 3 dB cutoff frequency of the filter should be kept minimum in order to simplify the filter design. It was found from the simulation that the filter which gives satisfactory raised cosine output pulse shape should be a seventh order Bessel lowpass filter with a 3 dB cutoff frequency equal to 1.3 times reciprocal of the pulsewidth. For the FSDD receiver which uses 325 Mbps QPPM signal format, the 3 dB cutoff frequency of the Bessel lowpass filter should be $1.3 \times (650 \times 10^6) = 845$ MHz.

Figure 3 shows a printout of the simulation results. The waveforms in the upper right graticule are the rectangular input pulse and the pulse output from the preamplifier. The waveforms in the lower graticule are the filter output and the true raised cosine pulse shape. The pulse output from the preamplifier is distorted somewhat due to the limited bandwidth of the preamplifier. Nevertheless, the pulse shape output from the Bessel lowpass filter had little improvement as the preamplifier bandwidth was increased. It is therefore sufficient for the preamplifier to have a bandwidth of the reciprocal of the pulsewidth. A slightly lower preamplifier bandwidth can be compensated by a higher 3 dB cutoff frequency of the Bessel lowpass filter. In practice, the 3 dB cutoff frequency of the Bessel lowpass filter should be determined after the preamplifier is chosen.

It was also found from the simulation that the lower 3 dB cutoff frequency due to the AC coupling should be no higher than 0.2% of the reciprocal of the input pulsewidth. For the FSDD receiver which uses 325 Mbps QPPM signal format, the lower 3 dB cutoff frequency due to AC coupling should not exceeds $650(MHz) \times 0.2\% = 1.3$ MHz. A higher cutoff frequency causes the pulses to overshot on the falling edge and consequently causes intersymbol interference.

Figure 4 shows an implementation of the Bessel lowpass filter according to [3]. The filter can be built with lumped components [4].

References

[1] F. M. Davidson, X. Sun, and M. A. Krainak, 'Bandwidth requirements for direct detection optical communication receivers with PPM signaling,' *Free-Space Laser Communication Technologies III,* David L. Bergley, Bernard D. Serry, Editors, Proc. SPIE 1417, pp. 75-88 (1991).

[2] H. J. Blinchikoff and A. I. Zverev, *Filtering in the Time and Frequency Domains,* John Wiley & Sons, New York, 1976.

[3] S. Niewiadomski, *Filter Handbook — a practical design guide,* CRC Press, Inc., Boca Raton, Florida, 1989, pp. 34-38.

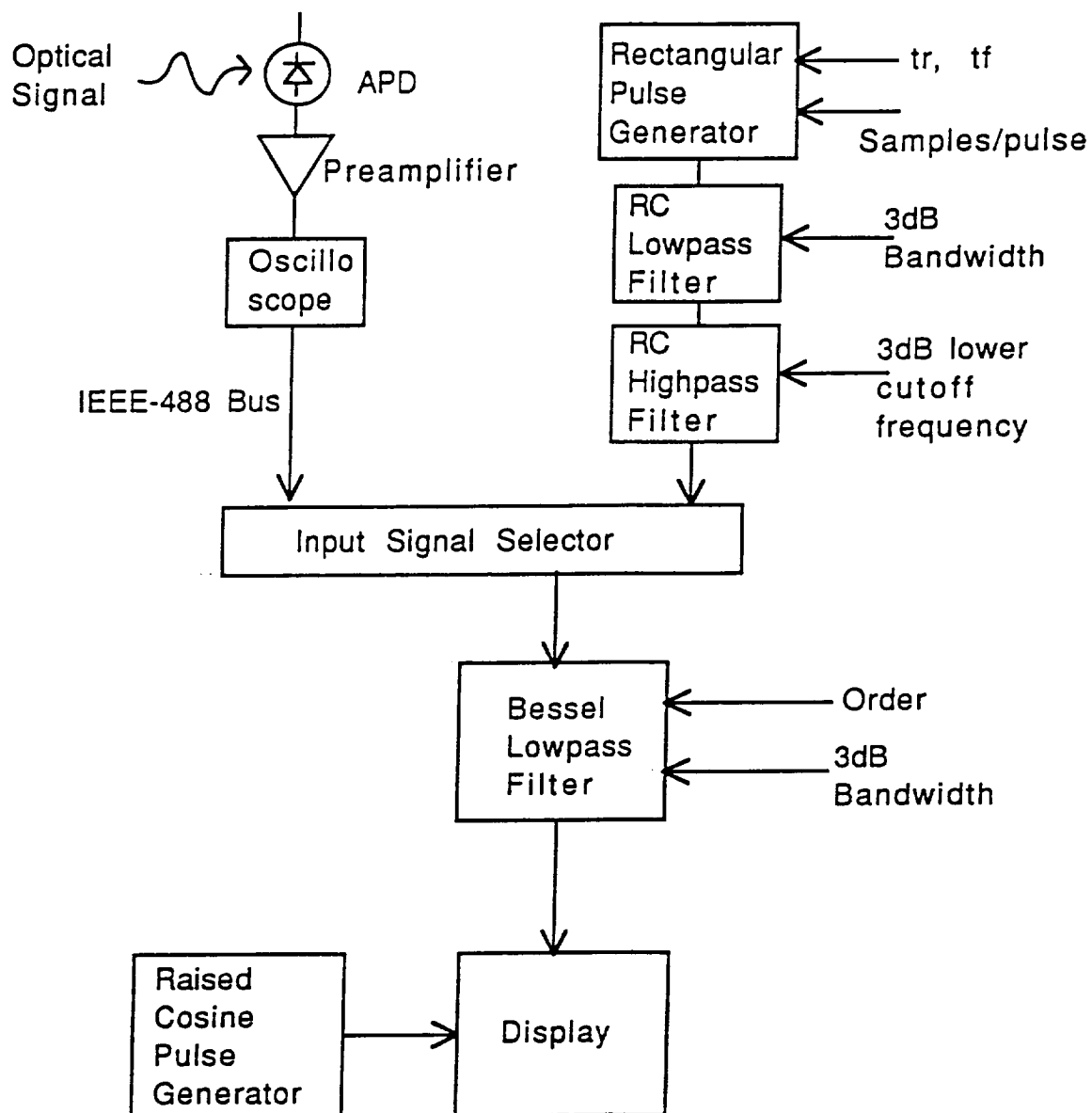[4] *RF and Microwave Filters,* K&L Microwave Inc., catalog, 1985.
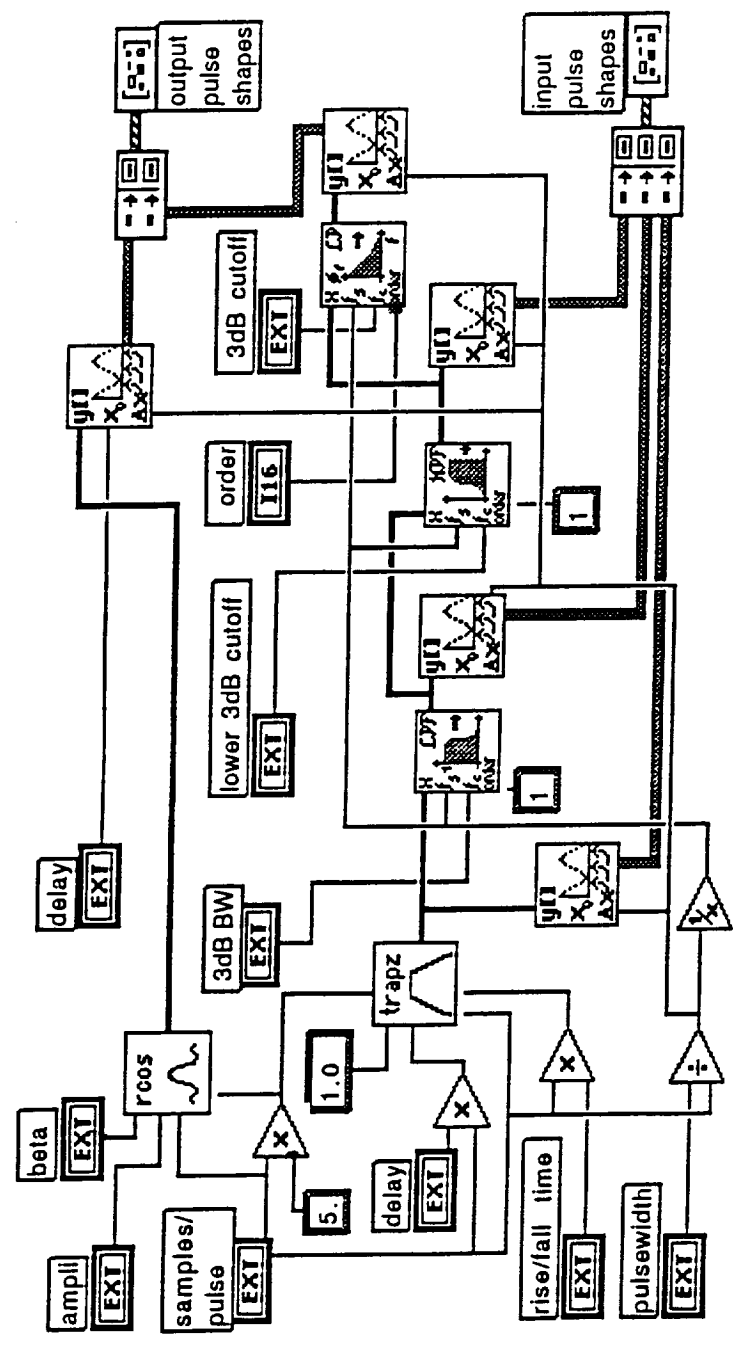
Figure 1. Block diagram of the program.

Block Diagram

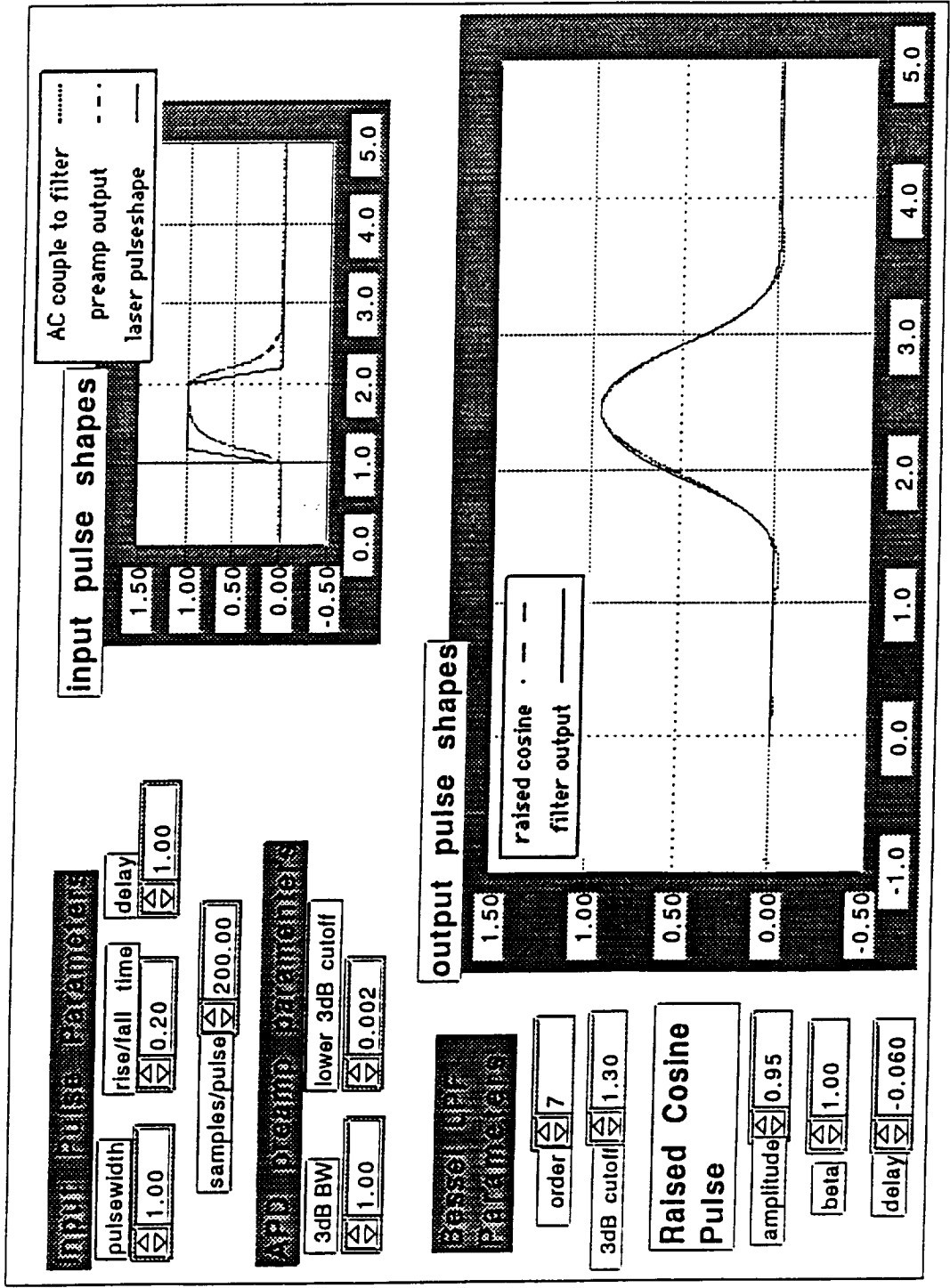
Figure 2.   Printout of the Program.

Front Panel

input pulse shapes

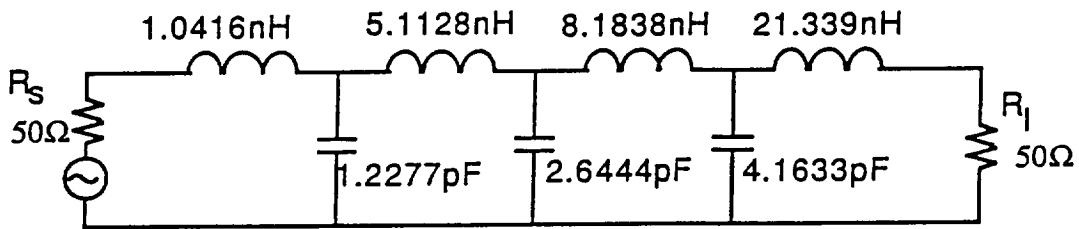AC couple to filter ....
preamp output - - -
laser pulseshape ———

1.50
1.00
0.50
0.00
-0.50

0.0   1.0   2.0   3.0   4.0   5.0

output pulse shapes

raised cosine - - -
filter output ———

1.50
1.00
0.50
0.00
-0.50

-1.0   0.0   1.0   2.0   3.0   4.0   5.0

input pulse parameters

pulsewidth ◁▷ 1.00
rise/fall time ◁▷ 0.20
delay ◁▷ 1.00
samples/pulse ◁▷ 200.00

APD preamp parameters

3dB BW ◁▷ 1.00
lower 3dB cutoff ◁▷ 0.002

Bessel filter parameters

order ◁▷ 7
3dB cutoff ◁▷ 1.30

Raised Cosine Pulse

amplitude ◁▷ 0.95
beta ◁▷ 1.00
delay ◁▷ -0.060

Figure 3.   printout of the simulation result.

.1106 H   .5429 H   .8690 H   2.2659 H

R_s
1Ω

.3259F   .7020F   1.1052F

R_l
1Ω
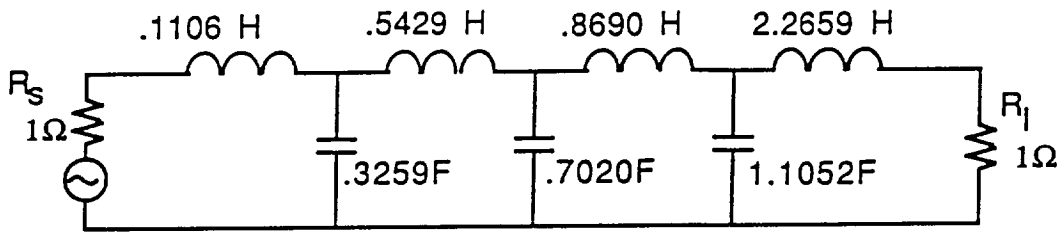
(a). Normalized 7th order Besses lowpass filter
($2\pi f_{3dB}$= 1 rad/sec., Rs=Rl=1Ω).

1.0416nH   5.1128nH   8.1838nH   21.339nH

R_s
50Ω

1.2277pF   2.6444pF   4.1633pF

R_l
50Ω

(b). Unnormalized 7th order Besses lowpass filter
(f_{3dB}=845MHz, Rs=Rl=50Ω)

Scalling: $C = C_n / 2\pi f_{3dB} R$, and $L = L_n R / 2\pi f_{3dB}$

Figure 4. A Circuit diagram of a 7th order Besses
lowpass filter [4].